Research Square

Preprints are preliminary reports that have not undergone peer review.
They should not be considered conclusive, used to inform clinical practice,
or referenced by the media as validated information.

Comparative Phylogenetic Resolution of 16S rRNA, hsp65, rpoB, and Multilocus Sequence Analysis for Identification of Clinical Mycobacterium Isolates

Gabriela Sevillano
Zurita & Zurita Laboratories
Jeannete Zurita
Zurita & Zurita Laboratories
José R. Ramírez-Iglesias
Universidad Internacional SEK
Camilo Zurita-Salinas
Zurita & Zurita Laboratories
Juan-Carlos Navarro
jcnavarro@uax.es

Universidad Alfonso X el Sabio (UAX), Villanueva de la Cañada

Article

Keywords: taxonomy, mycobacterial classification, phylogenetics, homology, clinical isolates, molecular identification, genotypic-phenotypic correlation

Posted Date: November 25th, 2026

DOI: https://doi.org/10.21203/rs.3.rs-11545937/v1

License: This work is licensed under a Creative Commons Attribution 4.0 International License. Read Full License

Additional Declarations: No competing interests reported.

Abstract

Background

Due to the differential treatment required by non-tuberculous mycobacteria (NTM) infections, accurate identification in clinical isolates is necessary for correct management, effective treatment, and appropriate control strategies. Traditional methods, including phenotypic tests, are slow, cumbersome, and often not definitive. PCR-based methods, such as restriction fragment length polymorphism analysis, are time-consuming and sometimes lead to inaccurate identification because they handle fragments of different sequences, but do not agree with their evolutionary origin. Sequencing is the most accurate method for species identification, with the 16S rRNA, *hsp*65, and *rpo*B genes being considered as candidates for phylogenetic and diagnostic studies.

Methods

We developed a phylogenetic analysis using the 16S rRNA, *hsp*65, and *rpo*B gene sequences of *Mycobacterium* clinical isolates, collected between 2018 and 2022, to assess their utility for taxonomic classification and identification of clinically relevant species. We also analyzed the genotype-phenotype correlation using sample origin, growth rate, and antimicrobial resistance. An alignment matrix was built (MacVector 18.5.8) based on the sequences generated in this study and sequences retrieved from NCBI, and phylogenetic analyses were performed using PAUP 4.0a. Futhermore, multilocus sequence analysis (MLSA) based on concatenated 16S rRNA, *hsp65*, and *rpoB* sequences was performed to improve phylogenetic resolution.

Results

The *rpo*B and *hsp*65 markers showed phylogenetic information at the level of groups of species and subspecies, whereas the 16S rRNA gene was the most conserved marker, yielding a structure at the species-complex level that can be used as a first level of identification. The concatenated analysis provided an improved overall phylogenetic topology and complementary species-level resolution compared with the individual-marker analyses. Clinical isolates showed phylogenetic homology with the *M. abscessus*, *M. avium*, *M. fortuitum*, and *M. intracellulare* groups. Synapomorphic characters varied among genes and showed genotype–phenotype correlations useful for understanding evolutionary trends and molecular identification for clinical purposes.

Conclusions

The combined analysis of 16S rRNA, *hsp65*, and *rpoB* genes provides improved phylogenetic resolution for the identification and classification of clinically relevant *Mycobacterium* species. The observed genotype–phenotype correlations contribute to understanding evolutionary relationships and may support the development of more accurate molecular identification methods with potential clinical and therapeutic applications.

1. Introduction

Nontuberculous mycobacteria species (NTM) are a group of environmental organisms that can be found in water, including drinking water, soil, animals, plants, food, vegetation, and human feces. These species have the potential to cause diverse pathologies, ranging from pulmonary, skin and soft tissue infections to deeper infections with or without systemic dissemination. Some NTM species are well-recognized pathogens, while others are only recently emerging, and their pathogenic potential remains unknown [1, 2].

Currently, diseases caused by NTM have increased compared to *Mycobacterium tuberculosis*. This may be related to the introduction of more sensitive laboratory techniques, the development of genomic techniques that allow faster diagnosis of mycobacterial diseases and a rapid differentiation of NTM [3]. More than 150 *Mycobacterium* species have been identified, with a fast pace increase in species identified due to the advancement of genetic techniques [4]. The progress of genetics and the development of mathematical models for analysis, in addition to the contribution of the global network of genetic sequences available in real time in public domain databases, have contributed to the advancement and more common use of phylogenetic analyses [5].

Phylogenetic and taxonomic studies of *Mycobacterium* species have been largely based on the analysis of the 16S RNA gene. Its high information content, conserved nature and presence in all organisms have made this gene a suitable candidate for phylogenetic analysis and identification. However, some limitations persist, mainly the genetic similarity (greater than 94%) that exists between species of the genus *Mycobacterium* [6]. For this reason, the combination of molecular marker analysis, such as *rpo*B and *hsp*65, together with the analysis of the 16S rRNA gene, has become an effective system for identifying mycobacterial species [7]. The 65 kDa heat shock protein gene (*hsp*65), highly conserved among mycobacterial species with hypervariable regions [8], and the *rpo*B gene, which encodes the β-subunit of RNA polymerase and contains regions of conserved sequences flanking highly variable regions, are used as alternative or complementary tools to identify mycobacteria [9].

Correct identification of NTM species is important for selecting the appropriate treatment for patients or epidemiological purposes [10]. Treatment depends on the specific NTM species and may range from the use of one or more antimicrobials, anti-tuberculous agents, to surgical debridement. Therefore, most NTM isolates should be identified at the species level and not only as species groups, both for treatment and to establish whether it is a colonizer of the clinical specimen or a true pathogen [11].

NTM species are traditionally classified by their growth rates into rapidly growing mycobacteria (RGM) and slowly growing mycobacteria (SGM) based on the time required for visible colony formation. Species that produce visible colonies on subculture plates within 3–7 days are classified as RGM, whereas those that take longer than 7 days are classified as SGM [12].

Because NTMs are a heterogeneous group of microorganisms, drug susceptibility greatly varies within species [13]. Currently, treatment of almost all RGM infections includes antibiotics such as macrolides (clarithromycin, azithromycin), sulfas (trimethoprim-sulfamethoxazole), aminoglycosides (amikacin, tobramycin), quinolones (moxifloxacin, ciprofloxacin), oxazolidinones (linezolid), cephamycins (cefoxitin), carbapenemics (imipenem), and tetracyclines (minocycline, doxycycline and tigecycline). While for infections caused by the SGM group, the regimen additionally includes ethambutol, isoniazid, streptomycin, and rifampicin (anti-tuberculous) [14].

Differences in antimicrobial susceptibility that determine treatment options among different mycobacteria mean that identification of NTMs to the species level is becoming increasingly important clinically. Mycobacterial susceptibility testing, therefore, is important for appropriate patient management and should be performed on clinically significant isolates of certain NTMs [11].

Although intraspecific and interspecific variations among mycobacteria from different geographic regions have been extensively studied using DNA sequences of 16S rRNA, *rpo*B and *hsp*65 genes, for ecological genetic studies, phylogenetic and evolutionary analyses, there is a lack of information on genetic variation among mycobacteria isolated from populations from various geographic regions, where mycobacterial infection is a major health problem [15]. Similarly, Ecuador has limited information on the genetic and epidemiological diversity of mycobacteria isolated from human samples [16, 17] and in greater proportion in environmental NTM [18].

Therefore, in this study, we propose to develop a phylogenetic analysis using 16S rRNA, *hsp*65 and *rpo*B gene sequences for taxonomic categorization and accurate species identification, genotype-phenotype correlation and understanding of the distribution and phylogenetic structure of NTM isolated from clinical samples from a private laboratory in the city of Quito, Ecuador.

2. Materials and Methods

2.1. Samples/sequences selected for the study

We obtained 57 previously isolated strains of the genus *Mycobacterium* from the biobank Microbiology Service of Zurita & Zurita Laboratories, a private clinical laboratory in Quito, Ecuador, during 2018–2022. The strains comprised isolates recovered from respiratory and non-respiratory specimens.

For the purpose of this study, the previously isolated and identified strains were thawed and subcultured on chocolate agar medium for rapid-growing strains and on Lowenstein-Jensen medium for slow-growing strains and incubated at 35°C with 5% CO2. Incubation time varied based on each species' growth characteristics.

We performed definitive identification by molecular methods using 16S rRNA, *rpo*B, and *hsp*65 gene sequencing. We entered the sequences into NCBI for preliminary identification; however, in some cases, we could not definitively identify closely related species. Therefore, we subjected all species to phylogenetic analysis.

Fisher's test was used to evaluate differences in the data for the different mycobacterial species analyzed. Statistical significance was set at $p < 0.05$. Analyses were performed in Past4.06b [19].

2.2. Antimicrobial resistance analysis

Antibiotic resistance testing was evaluated using the broth microdilution technique (MIC) with Sensititre system plates (Thermo Fisher Scientific, USA) for slow-growing NTM (SLOMYCO) and rapid-growing NTM (RAPMYCO), according to the manufacturer's recommendations [10]. Antimicrobial concentrations and dilution ranges were those predefined in the commercial RAPMYCO and SLOMYCO Sensititre panels according to the manufacturer’s specifications.

The antibiotics tested for RGM were trimethoprim/sulfamethoxazole, amikacin, clarithromycin, moxifloxacin, ciprofloxacin, linezolid, doxycycline, tigecycline, tobramycin, imipenem, minocycline, amoxicillin/clavulanic acid, cefepime, ceftriaxone, and for SGM were: trimethoprim/sulfamethoxazole, amikacin, clarithromycin, moxifloxacin, ciprofloxacin, linezolid, doxycycline, ethambutol, streptomycin, ethionamide, isoniazid, rifabutin, and rifampicin. The interpretation was performed according to CLSI guidelines [20]. Many mycobacteria do not have established breakpoints, therefore, in addition to the CLSI, other guidelines were used [21]. The antibacterial resistance index (ARI) was calculated to assess resistance in the different mycobacterial species identified [22]. This index relates pathogen susceptibility and antibiotic use to represent the overall level of resistance and efficacy of antibiotic therapy [23].

2.3. Genomic extraction, amplification and sequencing

Genomic DNA was extracted using the QIAamp DNA Minikit kit (QIAgen, Hilden, Germany) directly from chocolate agar medium or Lowenstein-Jensen's medium once NTMs formed visible colonies. Procedures and reagents were used according to the manufacturer's protocol. Eluted DNA was stored at -20°C until PCR analysis. Amplification of 16S rRNA, *rpo*B and *hsp*65 genes was performed. The primers for amplification and the expected amplicon sizes are listed in Table 1.

Table 1
Primers used for 16S rRNA, rpoB and hsp65 gene amplification.

Genes	Primers	Sequence	Fragment size	Reference
*hsp*65	**TB 11**	ACCAACGATGGTGTGTGTCCT	400 bp	[8]
	TB 12	CTTGTCGAACCGCATACC		
16S rRNA	**27F**	AGAGTTTGATCMTGGCTCAG	1500 bp	[24]
	1492R	TACGGYTACCTTGTTACGACTT		
*rpo*B	**rpoB-R**	AGCGGCTGCTGGGCTGGGTGATCATC	720 bp	[9]
	rpoB-F	GGCAAGGTCACCCCCCGAAGGG		

The following cycling conditions were used: initial denaturation of 4 min at 95°C; 35 cycles of 30s at 95°C, 1 min at 60°C (*hsp*65), 55°C (*rpo*B), 57°C (16S rRNA), 1 min at 72°C; and a final extension of 10 min at 72°C. PCR products were visualized on 1.5% agarose gel electrophoresis under ultraviolet light.

The PCR products of the three genes were sequenced by the Sanger method using the same amplification primers, with the exception of the 16S rRNA gene, where primers 518F (5'-CCAGCAGCAGCCGCGGGGTAATACG-3') and 800R (5'-TACCAGGGTATCTAATCC-3') were used to cover the entire region [25].

2.4 Sequence alignment and BLAST

We aligned the sequences produced by the forward and reverse primers using Sequencher 5.4.6 (Gene Codes Corporation, Ann Arbor, MI, USA) to obtain a consensus sequence, labeled with the corresponding code. Consensus sequences were aligned against the NCBI GenBank database using the BLASTn local alignment tool to obtain preliminary identity assessments, including percent nucleotide similarity and coverage values (NCBI accession numbers below in the Data Availability Statement). We retrieved mycobacterial sequences for each marker (16S rRNA, *rpo*B, and *hsp*65) from NCBI. A total of 167 sequences were included: 53 for 16S rRNA, 57 for *rpo*B, and 57 for *hsp*65. We also incorporated sequences from related reference groups and outgroups, such as *Tsukamurella*, *Gordonia*, and *Nocardia* species [26]. **Supplementary Table 1** lists the *Mycobacterium* species and reference-group sequences used, along with sample origins and NCBI accession numbers.

An alignment matrix was constructed for each gene or marker using ClustalW in MacVector software 18.5.8 with Gap Creation Penalty-GOP and Gap Extension Penalty-GEP parameters of 30.0 and 10.0, respectively, looking for the highest degree of positional homology.

2.5 Phylogenetic Analysis

The respective aligned matrices were used for the phylogenetic hypothesis reconstruction as a second level of identification, using PAUP 4.0a (build 169) software for Maximum Parsimony (MP) optimization [27] and MEGAX for Maximum Likelihood (ML) were conducted using MEGA version X [28] of the 16S rRNA, *rpo*B and *hsp*65 genes.

The nucleotide substitution model of each matrix for ML analysis was calculated by Model Test under MEGAX, calculated by Akaike's criterion, and Bayesian Information Criterion (BIC). The ML tree was constructed with an initial MP tree and the respective model for each matrix-gene-marker.

MP construction was performed with 1,000 replicates of random addition of taxa and characters and branch swapping with TBR (Tree Bisection and Reconnection). Subsequently, homologous character reweighting was performed using the recalculated consistency index (RCI) and values. The branch support (in percentages) was obtained using 1,000 bootstrap pseudoreplicates of the matrix as a posteriori statistical support of clades or branches. The sequence of analyses is based on previous work [26]. A multilocus sequence analysis (MLSA) was subsequently performed by concatenating the aligned 16S rRNA, *hsp65*, and *rpoB* sequences for each isolate and reference strain. The concatenated dataset was subjected to phylogenetic reconstruction using the same MP and ML approaches to assess whether the combined loci improved phylogenetic resolution and species-level identification compared with individual-gene analyses.

As a third level of verification of molecular identification and for purposes of classification into complexes, groups, and verification of phylogenetic species (phylogenetic species concept), each monophyletic clade was evaluated by inter- and intra-clade divergence through the construction of distance matrices using the uncorrected p-distance model, as well as between sequences obtained from NCBI and those obtained in the laboratory.

3. Results

3.1. Study population

Sensitivity profile data, the nature of the clinical specimen, growth type, and year of collection were collected for all 57 previously isolated mycobacterial strains. Most mycobacteria were isolated from respiratory specimens (31/57; 54.4%), followed by skin and soft tissues (25/57; 43.8%) and an effusion (1/57; 1.8%).

Of 57 samples, three (3/57; 5.26%) were identified as *M. tuberculosis* and 54 (94.74%) as NTM by phenotypic methods. In 24.56% (14/57) of the cases, NTMs were classified as SGM, and 70.17% (40/57) as RGM.

3.2. Antimicrobial resistance analysis

3.2.1. Analysis of antimicrobial resistance in RGMs

All isolates were subjected to susceptibility testing. Amikacin was the most active drug against RGM. No isolates were resistant to amikacin. A single isolate was resistant to tigecycline. For clarithromycin, 7.5% (3/40) of RGM were resistant. The resistance rate to linezolid was 42.5%. Resistance rates to amoxicillin/clavulanic acid, cefepime, and ceftriaxone showed 100% resistance in all isolates in the RGM group. Resistance rates to minocycline (32/40; 80%), imipenem (25/40; 62.5%), tobramycin (27/40; 67.5%), doxycycline (32/40; 80%), ciprofloxacin (33/40; 82.5%), moxifloxacin (20/40; 50%), and trimethoprim/sulfamethoxazole (25/40; 62.5%) were high for RGM (Table 2).

Table 2
Susceptibility profile of rapid-growing mycobacteria using

Rapid-growing mycobacteria								
Strain (n)	**Susceptibility**	**Trimethoprim/sulfamethoxazole n (%)**	**Amikacin n (%)**	**Clarithromycin n (%)**	**Moxifloxacin n (%)**	**Ciprofloxacin n (%)**	**Linezolid n (%)**	**Doxyc n (%)**
Mycobacterium abscessus subsp. abscessus (22)	Susceptible	11 (50%)	22 (100%)	20 (90.9%)	9 (40.9%)	0 (0%)	13 (59.1%)	1 (4.5
	Resistant	11 (50%)	0 (0%)	2 (10%)	13 (59%)	22 (100%)	9 (40.9%)	21 (95
Mycobacterium abscessus subsp. massiliense (5)	Susceptible	0 (0%)	5 (100%)	5 (100%)	1 (20%)	1 (20%)	3 (60%)	1 (20%
	Resistant	5 (100%)	0 (0%)	0 (0%)	4 (80%)	4 (80%)	2 (40%)	4 (80%
Mycobacterium abscessus subsp. bolletii (1)	Susceptible	1 (100%)	1 (100%)	1 (100%)	0 (0%)	0 (0%)	0 (0%)	0 (0%)
	Resistant	0 (0%)	0 (0%)	0 (0%)	1 (100%)	1 (100%)	1 (100%)	1 (100
Mycobacterium chelonae (7)	Susceptible	0 (0%)	7 (100%)	7 (100%)	5 (71.4%)	1 (14.3%)	5 (71.4%)	3 (42.
	Resistant	7 (100%)	0 (0%)	0 (0%)	2 (28.6%)	6 (85.7%)	2 (28.6%)	4 (57.
Mycobacterium conceptionense (2)	Susceptible	0 (0%)	2 (100%)	2 (100%)	2 (100%)	2 (100%)	0 (0%)	2 (100
	Resistant	2 (100%)	0 (0%)	0 (0%)	0 (0%)	0 (0%)	2 (100%)	0 (0%)
Mycobacterium fortuitum (3)	Susceptible	3 (100%)	3 (100%)	2 (66.7%)	3 (100%)	3 (100%)	2 (66.7%)	2 (66.

3.2.2. Analysis of antimicrobial resistance in SGMs

Resistance to clarithromycin was not observed in any isolate. Resistance rates to ciprofloxacin (6/14; 42.8%), linezolid (6/14; 42.8%), trimethoprim/sulfamethoxazole (5/14; 35.7%), moxifloxacin (5/14; 35.7%), ethionamide (4/14; 28.6%), rifabutin (3/14; 21.4%), amikacin (2/14; 14.3%), rifampicin (2/14; 14.3%), ethambutol (2/14; 14.3%), were less than 50% with the exception of streptomycin (7/14; 50%), isoniazid (7/14; 50%) and doxycycline (11/14; 78.6%) (Table 3).Differences were observed between the two types of mycobacteria in terms of the ARI (0.54 vs. 0.25). RGM showed a higher rate of resistance compared to SGM. The 3 subspecies of *M. abscessus* showed the highest rate of resistance among RGM in terms of the ARI (0.65). Within the SGM group, strains belonging to *M. avium* exhibited a higher resistance rate, as indicated by the ARI (0.41). After analysis of the ARI, *M. abscessus-chelone* complex showed a higher value than the other complexes, with a value of 0.61.

Table 3
Susceptibility profile of slow-growing mycobacteria using the Sensiti

Slow-growing mycobacteria								
Strain (n)	**Susceptibility**	**Trimethoprim/sulfamethoxazole n (%)**	**Amikacin n (%)**	**Clarithromycin n (%)**	**Moxifloxacin n (%)**	**Ciprofloxacin n (%)**	**Linezolid n (%)**	**Doxyc n (%)**
Mycobacterium marinum (1)	Susceptible	1 (100%)	1 (100%)	1 (100%)	1 (100%)	1 (100%)	1 (100%)	0 (0%
	Resistant	0 (0%)	0 (0%)	0 (0%)	0 (0%)	0 (0%)	0 (0%)	1 (10
Mycobacterium avium subsp hominissuis (7)	Susceptible	4 (57.1%)	6 (85.7%)	7 (100%)	3 (42.8%)	3 (42.8%)	2 (28.6%)	2 (28.
	Resistant	3 (42.9%)	1 (14.3%)	0 (0%)	4 (57.1%)	4 (57.1%)	5 (71.4%)	5 (71.
Mycobacterium avium complex (1)	Susceptible	0 (0%)	0 (0%)	1 (100%)	1 (100%)	1 (100%)	1 (100%)	1 (10
	Resistant	1 (100%)	1 (100%)	0 (0%)	0 (0%)	0 (0%)	0 (0%)	0 (0%
Mycobacterium intracellulare (2)	Susceptible	2 (100%)	2 (100%)	2 (100%)	2 (100%)	2 (100%)	2 (100%)	0 (0%
	Resistant	0 (0%)	0 (0%)	0 (0%)	0 (0%)	0 (0%)	0 (0%)	2 (10
Mycobacterium intracellulare complex (3)	Susceptible	2 (66.7%)	3 (100%)	3 (100%)	2 (66.7%)	1 (33.3%)	2 (66.7%)	0 (0%
	Resistant	1 (33.3%)	0 (0%)	0 (0%)	1 (33.3%)	2 (66.7%)	1 (33.3%)	3 (10

3.3 Molecular identification by phylogenetic analysis

Phylogenetic trees of the three 16S rRNA, *rpo*B and *hsp*65 genes were constructed, first from the genes separately and then using the concatenated data from a single alignment data set. All trees were rooted using the sequences of *Nocardia*, *Gordonia and Tsukamurella* species as outgroups, forming a monophyletic and basal group concerning *Mycobacterium* species, which were internally placed in a monophyletic group. The topologies and most of the interrelationships between *Mycobacterium* species were very similar and consistent in all the trees constructed, as well as the MP and ML results.

3.3.1. 16S rRNA gene phylogenetic analysis

For the construction of the phylogenetic tree based on the 16S rRNA gene, an alignment matrix of 1400 base pairs or positional characters by 102 sequences or taxa was used. The resulting tree is shown in Fig. 1. It was possible to observe the grouping of the *Mycobacterium* members into four main clades. Two of these clades are composed of slow-growing species, while the other two clades are composed of rapid-growing species. Within the clade of rapid-growing species, the basal subclade corresponds to the group we refer to as "*Fortuitum*", which encompasses most of the other rapid-growing species and the inner or derived subclade as "*Abscessus-Chelonae*". Relationships among species in the "*Fortuitum*" subclade were difficult to discern, unlike members of the "*Abscessus-Chelonae*" subclade, which formed a monophyletic lineage with a bootstrap value of 100% within the other rapid-growing *Mycobacterium* species and comprises the deepest-branching lineage among *Mycobacterium* species. For the case of *M. phlei*, *M. thermoresistible* and *M. monacense* species, which compose the rapid-growing species and belong to the subclade "*Fortuitum*", the formation of an earlier branching lineage within the genus *Mycobacterium* was observed.

Of the two clades of slow-growing mycobacteria, the subclade designated as "*Tuberculosis-Avium*" contains most of the clinically important mycobacterial species, such as *M. tuberculosis* and *M. avium*; and the "*Terrae*" subclade, which forms a sister and derivative clade with the "*Tuberculosis-Avium*" subclade.

The percentage of divergence of the 16S rRNA sequences within each subclade was low; the species of the "*Terrae*" subclade had a value of 1.46%, of the "*Tuberculosis-Avium*" subclade a value of 1.23%, of the "*Abscessus-Chelonae*" subclade a value of 0.93%, and of the "*Fortuitum*" subclade a value of 1.15%. For the case of complexes, the divergence percentages were for *M. tuberculosis* complex 0.35%, *M. avium* complex 0.079%, *M. intracellulare* complex 0.20%, *M. abscessus-chelonae* complex 0.20% and *M. fortuitum* complex 0.1%.

The divergence between *M. tuberculosis* and *M. avium* complexes was 1.80%, between *M. tuberculosis* and *M. intracellulare* was 2%, between *M. avium* and *M. intracellulare* was 0.6% and the divergence between *M. abscessus-chelonae* and *M. fortuitum* complexes was 3.97%.

Of the 57 clinical isolates analyzed, 53 yielded sequences of sufficient quality for 16S rRNA gene analysis, whereas four isolates were excluded. Of the 53 samples analyzed using the 16S rRNA gene, only three isolates were identified to species level: sample L572 as *M. marinum*, L535 as *M. chelonae* and L39 as *M. fortuitum*. The other isolates were identified at the complex or group level, the most predominant being *M. abscessus-chelonae* complex

3.3.2. *rpo*B gene analysis

For the *rpo*B gene, an alignment matrix comprising 720 nucleotide positions across 102 sequences (taxa) was used. Phylogenetic analysis of this region yields a different topology than that obtained from the 16S rRNA gene. The *rpo*B gene tree based on the mycobacterial is shown in Fig. 2.

In the *rpo*B tree topology, *Mycobacterium* is shown as a monophyletic clade with respect to the reference groups. The formation of two supported and differentiated monophyletic groups was observed. Group A is formed by the species belonging to the *M. tuberculosis*, *M. avium-intracellulare* and *M. fortuitum* complexes and group B is formed by the species of the *M. abscessus-chelonae* complex, which shows an earlier branching within the genus *Mycobacterium*.

This species location on the tree is related to antibiotic susceptibility; thus, the species belonging to *M. abscessus-chelonae* complex with a higher ARI value form a separate clade with respect to the other mycobacterial species (Fig. 2).

The *rpo*B gene could not differentiate among subspecies or variants within the different mycobacterial complexes. An exception was the *M. abscessus* complex, in which *M. chelonae* was clearly distinguished from the *M. abscessus* complex. However, differentiation among subspecies within the *M. abscessus* complex was not achieved, with *M. bolletii* and *M. massiliense* clustering together as *M. bolletii/massiliense*. Only *M. abscessus subsp. abscessus* formed a well-supported monophyletic group with the related isolates (bootstrap = 100%). The percentage of sequence divergence among species within each complex was 1.54% for the *M. tuberculosis* complex, 0.33% for the *M. avium* complex, 0.80% for the *M. intracellulare* complex, 2.76% for the *M. abscessus–chelonae* group, and 3.20% for the *M. fortuitum* complex.

The divergence between *M. tuberculosis* and *M. avium* complexes was 14.89%, between *M. tuberculosis* and *M. intracellulare* was 14.61%, between *M. avium* and *M. intracellulare* was 5.6%, and the divergence between *M. abscessus-chelonae* and *M. fortuitum* complexes was 12.28%.

Of the 57 clinical isolates analyzed, 36 were identified at the species level. Among these, 26 were identified as *M. abscessus* subsp. *abscessus*, two as *M. chelonae*, three as *M. fortuitum*, one as *M. marinum*, and two as *M. avium* subsp. *hominissuis*. Two additional isolates were identified as *M. abscessus*; however, the gene did not provide sufficient resolution to discriminate among the closely related subspecies *M. massiliense*, and *M. bolletii*. The remaining isolates were assigned only to the corresponding species complex or group.

3.3.3. *hsp*65 gene analysis

Finally, the analysis was performed with the *hsp*65 gene, using an alignment matrix of 400 base pairs or positional characters for 105 sequences or taxa. It is possible to visualize the formation of two clearly defined groups: those belonging to the *M. abscessus-chelonae* complex, *M. tuberculosis*, *M. avium*, *M. intracellulare*, and the second group formed by the *M. fortuitum* complex that presents a more basal branching (Fig. 3). After the statistical analysis of the demographic characteristics, it was identified that the clade differentiation could be related to the type of sample, obtaining that the species belonging to the clade A are more frequently isolated from respiratory samples, while those of the clade B are mainly isolated from non-respiratory samples (p = 0.0157).

The percentage of divergence of species within complexes for *M. tuberculosis* had a value of 1.68%, *M. avium* a value of 0.11%, *M. intracellulare* a value of 1.10%, *M. abscessus-chelonae* a value of 2.98% and *M. fortuitum* a value of 2.10%. The divergence between *M. tuberculosis* and *M. avium* complexes was 7.02%, between *M. tuberculosis and M. intracellulare* was 7.46%, between *M. avium* and *M. intracellulare* was 4.16% and the divergence between *M. abscessus-chelonae* and *M. fortuitum* complexes was 6.90%.

Thirty-six (36/57; 63.15%) isolates belonging to the *M. abscessus–chelonae* group, which represented the most prevalent phylogenetic group. Among these, 29 isolates belonged to *M. abscessus* complex, including *M. abscessus subsp. abscessus* (n = 22), *M. abscessus subsp. massiliense* (n = 6), and *M. abscessus subsp. bolletii* (n = 1), whereas seven isolates were identified as *M. chelonae*.

Three isolates were assigned to the *M. tuberculosis* complex; however, the available sequence data did not allow differentiation among the individual species within this complex. Within the *M. intracellulare* complex, four isolates were assigned to the complex level, of which only two were resolved to the species level as *M. intracellulare*. Within the *M. avium* complex, nine isolates were assigned to the complex level, of which eight were resolved as *M. avium subsp. hominissuis*.

Within the *M. fortuitum* complex, four isolates were identified, and species-level differentiation was achieved for all of them, with two isolates identified as *M. conceptionense* and two as *M. fortuitum*. In addition, one isolate was identified as *M. marinum*.

3.3.4. Multilocus sequence analysis (MLSA) based on concatenated 16S rRNA, *hsp65*, and *rpoB* sequences

Another phylogenetic tree was constructed based on the concatenated sequences of the three genes analyzed. The concatenated analysis improved the overall phylogenetic resolution and provided consistent species-level identification, including for isolates belonging to the '*Fortuitum*' clade (Fig. 4). It was not possible to differentiate between the subspecies *M. bolletii* and *M. massiliense*. The topology was similar to that of the phylogenetic tree obtained with the *rpo*B gene.

Sequence divergence within each complex was 1.09% for *M. tuberculosis*, 0.15% for *M. avium*, 0.62% for *M. intracellulare*, 1.29% for *M. abscessus-chelonae* and 2.26% for *M. fortuitum*. The divergence between *M. tuberculosis* and *M. avium* complexes was 5.72%, between *M. tuberculosis* and *M. intracellulare* was 5.87%, and between *M. avium* and *M. intracellulare* was 2.37%. Finally, the divergence between *M. abscessus-chelonae* and *M. fortuitum* complexes was 6.4%.

In the concatenated analysis, several isolates were resolved at the species or subspecies level. *M. chelonae* was identified in seven isolates (bootstrap support, 78%), *M. fortuitum* in three isolates (58%), *M. conceptionense* in two isolates (96%), and *M. abscessus* subsp. *abscessus* in 24 isolates (70%). One isolate was assigned to the *M. abscessus–M. massiliense* group, one to *M. marinum* (100%), and three to *M. intracellulare* (91%).

At the species-complex level, two isolates were assigned to the *M. tuberculosis* complex, nine to the *M. avium* complex, and four to the *M. intracellulare* complex.

Among the three genes analyzed, the *hsp*65 typing method showed better agreement for species- and subspecies-level identification, whereas the concatenated analysis provided superior overall phylogenetic topology.

The concatenated analysis resolved some of the paraphyletic placements observed in the individual gene analyses, particularly within the '*Fortuitum*' and '*Terrae*' subclades, resulting in an improved overall phylogenetic topology. However, MLSA did not improve discrimination in all groups, as *M. bolletii* and *M. massiliense* remained unresolved in the concatenated tree, whereas *hsp*65 alone provided greater discriminatory resolution for these subspecies.

4. Discussion

The incidence of NTM infections in clinical specimens has increased in several regions of the world, so the immediate diagnosis and clear and accurate identification of NTM species causing the disease has become a necessity [29]. In Ecuador, the incidence of atypical mycobacteria in clinical specimens is unknown and the only available data are case reports of some species, including *M. scrofulaceum* [30], *M. terrae* [31], *M. abscessus subsp. abscessus* [32], *M. timonense* [17] and *M. monacense* [33]. Therefore, the present study proposes a way to accurately identify mycobacteria and determine the diversity of species isolated from clinical samples.

Molecular techniques have enabled accurate, rapid, and reliable identification of mycobacterial species, with whole-genome sequencing regarded as the gold standard for NTM identification [34]. However, these approaches are expensive, require specialized expertise, and are not readily available in routine laboratories in resource-limited contexts [35]. As an alternative, sequencing of highly conserved yet hypervariable regions, such as the 16S rRNA (~ 1500 bp), *rpo*B (~ 3500 bp), and *hsp*65 (~ 1600 bp) genes, has become more widespread in diagnostic workflows [36]. Many studies have focused on partial regions within these genes that balance sufficient conservation with intraspecies variability to achieve accurate identification while reducing costs. In our study, we analyzed the full-length 16S rRNA gene (1500 bp), a 400 bp fragment of *hsp*65 [8], and a 720 bp fragment of *rpo*B [9].

Phylogenetic analysis of 16S rRNA, *rpo*B and *hsp*65 generally showed topologically similar trees. In the case of the 16S rRNA tree, clades comprising most of the slow-growing mycobacteria were clearly differentiated from the rapid-growing species. This differentiation is evident due to the insertion of 12 to 14 nucleotides in the 16S rRNA sequences in SGM, which are often used as a marker to differentiate between RGM and SGM [37]. In the analysis performed in this study, a 12-nucleotide insertion was observed in SGM mycobacteria belonging to the "*Tuberculosis*" subclade, and a 14-nucleotide insertion belonging to mycobacteria of the "*Terrae*" subclade (Fig. 1).

Regarding the phylogenetic analysis of the *rpo*B gene, the *M. abscessus-chelonae* complex separated from the *M. fortuitum* complex, forming a separate clade. This differentiation may be related to resistance characteristics, as species in the *M. abscessus–chelonae* complex exhibit higher ARI values than other mycobacteria. Being members of the *M. abscessus-chelonae* complex, belonging to group B, the bacteria with higher resistance rates compared to mycobacteria grouped with group A [38, 39] [45, 46] (Fig. 2). Statistical analyses of antimicrobial resistance profiles showed that members of the *M. abscessus-chelonae* complex presented the highest ARI (0.61) with respect to the other species. This phenotype has generally been attributed to mycobacterial envelope impermeability, with the cell wall of *M. abscessus* and *M. chelonae* being 10 to 20 times less permeable than other mycobacteria, due to the higher lipid content, which coincides with *M. abscessus-chelonae* complex being the most resistant to antibiotics [40].

The *rpo*B gene contains additional useful information related to rifampicin susceptibility of a particular species (or strain) of mycobacteria [41]. Rifampicin resistance is largely associated with mutations in an 81 bp fragment of the *rpo*B gene, in addition to other mechanisms such as reduced cell wall permeability or an enhanced efflux pump [14].

RGM, with common representatives including *M. abscessus* [42] and *M. fortuitum* [43], exhibit intrinsic resistance to rifampicin. In contrast, SGM such as *M. tuberculosis* often develop acquired resistance mediated by mutations in the *rpo*B gene or by overexpression of efflux pumps [44]. Rifampicin resistance in *M. abscessus* is attributed to its distinctive cell wall, characterized by higher lipid content and the presence of ADP ribosyltransferases, rather than the *rpo*B mutations that predominate in many other mycobacteria [45]. Although *M. fortuitum* is classified as an RGM, rifampicin resistance in this species has also been linked to *rpo*B gene mutations similar to those observed in *M. tuberculosis*[46], which makes *M. fortuitum* a useful surrogate for *M. tuberculosis* in susceptibility testing studies. These differences in resistance phenotypes may reflect the clear phylogenetic separation observed between these species.

The divergence in the phylogenetic analysis of *rpo*B could also be related to the G + C% content in mycobacterial species. It is known that the *rpo*B gene allows an efficient estimation of bacterial G + C% content [46], therefore the species found in group A, corresponding to the *M. tuberculosis*, *M. avium*, *M. intracellulare* and *M. fortuitum* complexes, which present higher G + C% contents, with values of 65.6%, 69.1%, 68% [47] and 66% [48], respectively, formed a monophyletic group differentiated from members of group B species corresponding to the *M. abscessus-chelonae* complex that present the lowest G + C% values, with a value of 64.2% [49].

Finally, the *hsp*65 gene tree showed a clustering of the *M. abscessus-chelonae*, *M. tuberculosis*, *M. intracellulare* and *M. avium* complex species into a single clade separate from the *M. fortuitum* complex members. This structured topology between clades could be related to sample type or origin, which upon statistical analysis showed a statistically significant difference of clades vs. sample type ($p = 0.0157$), suggesting that there is a higher prevalence of species isolated from respiratory samples in clade A in contrast to clade B. Species of the *M. abscessus-chelonae* complex have been isolated more frequently from respiratory infections, a characteristic shared with the slow-growing mycobacteria, as opposed to *M. fortuitum*, which produces a wide variety of extrapulmonary diseases, 60% of cases being cutaneous infections [38]. It has been established that three species make up the vast majority of pulmonary infections by atypical mycobacteria; these are: *M. avium*, *M. kansasii* and *M. abscessus* [50], similar to the results obtained in our analysis.

The *hsp*65 gene encodes a virulence-associated protein that plays an important role in mycobacterial latency [51]. Accordingly, divergence observed in phylogenetic analyses of *hsp*65 may reflect the pathogenic potential within the genus *Mycobacterium*, dividing more pathogenic species into group A and less pathogenic species into group B. Slow-growing species, most notably *M. tuberculosis* and *M. leprae*, are generally the most pathogenic, whereas most rapidly growing species exhibit lower pathogenicity. An exception is *M. abscessus*, which, owing to its extensive repertoire of virulence factors, phenotypically resembles slow-growing pathogens [52]. For example, a comparative study of pulmonary disease caused by *M. abscessus* and *M. avium* highlighted

similarities in pathogenicity [38]. Moreover, at the cellular level, *M. abscessus* mimics features of pathogenic slow-growing mycobacteria, such as the ability to survive and replicate within macrophages. In contrast, *M. fortuitum* cannot multiply within macrophages and is rapidly cleared from infected cells [53].

Phylogenetic analyses yielded molecular identification of nine species using 16S rRNA, *rpo*B and *hsp*65 genes as molecular markers, with *M. abscessus subsp. abscessus* being the most prevalent species, followed by *M. chelonae* and *M. avium subsp hominissuis.* Not all molecular markers were able to reach species level identification, similar to the result reported by Ledesma et al., [26]. The *hsp*65 gene yielded optimal results in terms of species and subspecies identification.

Although the 16S rRNA gene is commonly used for bacterial identification and has a large amount of information in the NCBI database [54], for NTMs, the sequences show little interspecific variation, so it may not distinguish closely related species [26], with sequencing of the 16S rRNA region alone being insufficient [55]. In our study, only three isolates were identified to species level using the 16S rRNA gene: *M. marinum*, *M. chelonae*, and *M. fortuitum*.

In this study, the percentage of divergence between the *M. abscessus-chelonae*, *M. tuberculosis* and *M. bovis*, *M. fortuitum* complexes was lower using the 16S rRNA gene compared to *rpo*B and *hsp*65, which corroborates the difficulty in distinguishing the species using 16S rRNA sequences alone. Members of these complexes could be better distinguished by analysis of the *hsp*65 and *rpo*B genes.

The *rpo*B gene, which encodes the b subunit of RNA polymerase, has emerged as a candidate gene for phylogenetic analyses and identification of bacteria, especially when studying closely related strains [46]. Several studies have indicated that the hypervariable region of the *rpo*B, gene located between positions 2300 and 3300 is best suited for phylogenetic identification and discrimination at the species and subspecies level [46]. In our study, 36 isolates were identified to species level, 2 isolates as *M. chelonae*, 3 as *M. fortuitum*, 1 as *M. marinum* and 26 were identified as *M. abscessus* subsp. *abscessus*.

In the case of the closely related subspecies *M. abscessus*, *M. bolletii* and *M. massiliense*, the *rpo*B region alone was not sufficient for good discrimination [56]. Finding divergence values of 0.0% between *M. bolletii* and *M. massiliense* subspecies and 2.03% between *M. abscessus* and *M. bolletii*, *M. massiliense*. Between-group divergence values < 2% in *rpo*B sequences indicate that these groups belong to the same species [57]. This was more marked for *M. massiliense* and *M. bolletii*, than for *M. abscessus*. The *rpo*B sequences in the strains of the *M. massiliense* and *M. bolletii* groups did not diverge. Therefore, according to Adékambi et al. [57] criteria, *M. massiliense* and *M. bolletii* for this analysis do not constitute different species. The importance of correctly identifying the subspecies of *M. abscessus* lies in their antimicrobial profile. *M. abscessus* and *M. bolletii* are known to have inducible macrolide resistance due to the presence of the functional erm(41) gene, while *M. massiliense* is susceptible because this gene is truncated and non-functional [58]. Therefore, the correct identification of *M. abscessus* subspecies is of clinical relevance.

The hsp65 gene is a good option for the identification of RGM, because it shows more variability than the 16S rRNA and *rpo*B genes [59]. In this study, it was possible to identify the subspecies of M. abscessus by analyzing the *hsp*65 gene, obtaining a percentage of divergence of 0.64% between the subspecies *M. bolletii* and *M. massiliense*, 1.28% between *M. abscessus* and *M. massiliense* and 1.41% between *M. abscessus* and *M. bolletii*. This gene is part of the 60 kDa heat shock protein family and has been considered a useful phylogenetic marker in several bacterial genera, due to its highly conserved primary structures [60]. The presence of a single copy of the gene in the genome means that it is not easily transferred from one bacterium to another, unlike the *rpo*B gene [61], it is suitable for phylogenetic studies of species or closely related strains. Analysis based on the *hsp*65 gene identified 53 isolates to species level, seven belonging to *M. chelonae*, 29 to *M. abscessus* (22 to *M. abscessus*; 6 to *M. massiliense*; one to *M. bolletii*), three to *M. tuberculosis*, two to *M. intracellulare*, eight to *M. avium-hominissuis*, one to *M. marinum*, two to *M. conceptionense* and two *to M. fortuitum.*

Although *hsp65* showed the highest discriminatory capacity among the individual markers, particularly at the species and subspecies levels, analysis of a single locus may not fully reflect the evolutionary relationships among closely related taxa. Therefore, to improve phylogenetic resolution beyond that obtained with individual markers, a multilocus sequence analysis (MLSA) based on the concatenated 16S rRNA, *hsp*65, and *rpo*B sequences was performed.

The partial paraphyletic placement of some rapid-growing species belonging to the "*Fortuitum*" and "*Terrae*" subclades observed in the individual gene trees was resolved in the concatenated analysis, resulting in an improved overall phylogenetic topology. This finding supports the complementary value of combining multiple loci for resolving evolutionary relationships among closely related mycobacterial taxa. However, the MLSA approach did not improve discrimination in all groups, as *M. bolletii* and *M. massiliense* remained unresolved in the concatenated tree. In contrast, *hsp*65 alone showed greater discriminatory capacity for some closely related species and subspecies. Therefore, our results suggest that MLSA provides a more robust overall phylogenetic framework, whereas the discriminatory contribution of individual loci may vary according to the taxonomic group analyzed [37].

Limitations

The main limitations of this study are related to the phylogenetic resolution provided by the genetic markers analyzed and the unequal representation of some *Mycobacterium* species. Phylogenetic resolution was limited by the discriminatory power of the three markers analyzed, with the inclusion of additional loci, particularly *gyrB* and *recA*, potentially improving the resolution of closely related or unresolved *Mycobacterium* species. Whole-genome sequencing could provide further genomic resolution for isolates that remain unresolved using multilocus approaches. The low representation of some species also limited the statistical robustness of phylogenetic and genotype–phenotype comparisons. Larger and more balanced datasets, particularly including underrepresented species, are needed to validate the observed phylogenetic relationships and genotype–phenotype associations.

5. Conclusions

Synapomorphic characters (shared positional homologies of an immediate common ancestor) for the identification and reliable demarcation of different monophyletic clades of mycobacteria varied among genes analyzed, with correlation observed between the *hsp*65 gene and pathogenicity phenotypes and sample type, *rpo*B with resistance profile, G-C% content, and 16S rRNA with growth rate.

The 16S rRNA gene was more conserved and showed less variability compared to the *rpo*B and *hsp*65 genes. The *hsp*65 and *rpo*B genes showed greater variability, which allowed an optimal identification approach at the species level and even at the subspecies level, as in the case of the *hsp*65 gene. These phylogenetic results emphasize that molecular markers other than the 16S rRNA gene should be applied to obtain an accurate phylogenetic and evolutionary scheme, and concatenated analyses of genes with greater phylogenetic information at specific levels.

Clinical samples showed phylogenetic homology with the *M. abscessus–chelonae* group (*Mycobacterium abscessus* subsp. *abscessus*, *Mycobacterium abscessus* subsp. *massiliense*, *Mycobacterium abscessus* subsp. *bolletii*, and *M. chelonae*), the *M. avium* group (*Mycobacterium avium* subsp. *hominissuis*), and the *M. fortuitum* group (*M. conceptionense* and *M. fortuitum*), as well as with *M. intracellulare* and *M. marinum*.

These results support the complementary use of highly discriminatory individual markers, particularly *hsp*65, together with multilocus sequence analysis (MLSA) based on concatenated loci to improve the phylogenetic resolution of clinically relevant *Mycobacterium* specie.

Declarations

Ethics approval and consent to participate: Not applicable

Author Contributions:

"Conceptualization, JCN. and GS.; methodology, JCN.; software, JCN.; validation, JCN, GS. and JZ.; formal analysis, GS and JCN.; resources, JCN and JZ.; data curation, GS.; writing-preparation of original draft, GS.; writing-revision and editing, GS, JCN and JRRI.; final visualization, JCN and JRRI.; supervision, JCN and JZ.; administration and project management, JZ and JCN.; acquisition of funds, JZ and JCN. "All authors have read and agree to the final version of the manuscript."

Funding:

"This research was funded by DII-UISEK-P011617_(JCN, JRRI), Fundacion Universidad Alfonso X el Sabio (FUAX) 1.200.008 (JCN) and by the Biomedicine Research Unit of Zurita & Zurita Laboratorios".

Institutional Review Board Statement:

The mycobacteria samples come from the Zurita & Zurita Laboratories Biomedical Research Unit strain, which approved their use, and no patient data are included.

Data Availability Statement: The datasets generated and analyzed during the current study are available in the GenBank repository of the National Center for Biotechnology Information (NCBI). Individual gene sequences are available under accession numbers QB297045–QB297097 (16S rRNA); QB310402–QB310458 (*rpoB*) and QB315245–QB315301(*Hsp65*).

Acknowledgments: To the Microbiology area of Zurita & Zurita Laboratorios.

Conflicts of Interest: The authors declare that they have no conflicts of interest.

References

1. Rahama, O. & Thaker, H. Atypical mycobacteria: an important differential for the general physician. *Clin. Med. (Northfield Il)*. **13**, 504. https://doi.org/10.7861/CLINMEDICINE.13-5-504 (2013).
2. Eisenstadt, J. & Hall, G. S. Microbiology and classification of mycobacteria. *Clin. Dermatol.* **13**, 197–206. https://doi.org/10.1016/0738-081X(95)00021-7 (1995).
3. Field, S. K. & Cowie, R. L. Lung disease due to the more common nontuberculous mycobacteria. *Chest* **129**, 1653–1672. https://doi.org/10.1378/chest.129.6.1653 (2006).
4. Tortoli, E. Impact of genotypic studies on mycobacterial taxonomy: the new mycobacteria of the 1990s. *Clin. Microbiol. Rev.* **16**, 319–354. https://doi.org/10.1128/CMR.16.2.319-354.2003 (2003).
5. Faria, S., Joao, I. & Jordao, L. General Overview on Nontuberculous Mycobacteria, Biofilms, and Human Infection. *J. Pathog*. **2015**, 1–10. https://doi.org/10.1155/2015/809014 (2015).
6. Devulder, G., de Montclos, M. P. & Flandrois, J. P. A multigene approach to phylogenetic analysis using the genus Mycobacterium as a model. *Int. J. Syst. Evol. Microbiol.* **55Pt 1**, 293–302. https://doi.org/10.1099/IJS.0.63222-0 (2005).
7. Maleki, M. R., Kafil, H. S., Harzandi, N. & Moaddab, S. R. Identification of nontuberculous mycobacteria isolated from hospital water by sequence analysis of the hsp65 and 16S rRNA genes. *J. Water Health*. **15**, 766–774. https://doi.org/10.2166/WH.2017.046 (2017).
8. Telenti, A. et al. Rapid identification of mycobacteria to the species level by polymerase chain reaction and restriction enzyme analysis. *J. Clin. Microbiol.* **31**, 175–178. https://doi.org/10.1128/jcm.31.2.175-178.1993 (1993).
9. Adékambi, T., Colson, P. & Drancourt, M. rpoB-Based Identification of Nonpigmented and Late-Pigmenting Rapidly Growing Mycobacteria. *J. Clin. Microbiol.* **41**, 5699–5708. https://doi.org/10.1128/JCM.41.12.5699-5708.2003 (2003).
10. Huang, W. C., Yu, M. C. & Huang, Y. W. Identification and drug susceptibility testing for nontuberculous mycobacteria. *J. Formos. Med. Assoc.* **119**, S32–41. https://doi.org/10.1016/J.JFMA.2020.05.002 (2020).

11. Griffith, D. E. et al. An official ATS/IDSA statement: Diagnosis, treatment, and prevention of nontuberculous mycobacterial diseases. *Am. J. Respir Crit. Care Med.* **175**, 367–416. https://doi.org/10.1164/rccm.200604-571ST (2007).
12. Runyon, E. H. Typical Mycobacteria:Their classification. *Am. Rev. Respir Dis.* **91**, 288–289. https://doi.org/10.1164/ARRD.1965.91.2.288 (1965).
13. Zhou, L. et al. Trends in the Prevalence and Antibiotic Resistance of Non-tuberculous Mycobacteria in Mainland China, 2000–2019: Systematic Review and Meta-Analysis. *Front. Public. Heal*. **8**, 295. https://doi.org/10.3389/fpubh.2020.00295 (2020).
14. Saxena, S., Spaink, H. P. & Forn-Cuní, G. Drug Resistance in Nontuberculous Mycobacteria: Mechanisms and Models. *Biology (Basel)*. **10**, 1–22. https://doi.org/10.3390/BIOLOGY10020096 (2021).
15. Hoefsloot, W. et al. The geographic diversity of nontuberculous mycobacteria isolated from pulmonary samples: an NTM-NET collaborative study. *Eur. Respir J.* **42**, 1604–1613. https://doi.org/10.1183/09031936.00149212 (2013).
16. Echeverria, G. et al. First Case Reports of Nontuberculous Mycobacterial (NTM) Lung Disease in Ecuador: Important Lessons to Learn. *Pathog (Basel Switzerland)*. 12. https://doi.org/10.3390/PATHOGENS12040507 (2023).
17. Zurita, J. et al. Characterization of the first report of Mycobacterium timonense infecting an HIV patient in an Ecuadorian hospital. *Clin. Microbiol. Infect.* **20**, O1113–O1116. https://doi.org/10.1111/1469-0691.12675 (2014).
18. Orlando, S. A. et al. Non-tuberculous mycobacteria and other acid fast bacilli pathogens identification by qPCR and MALDI-ToF MS in tuberculosis-like lesions of slaughtered cattle from Ecuador. *Front. Vet. Sci.* **12**, 1565066. https://doi.org/10.3389/fvets.2025.1565066 (2025).
19. Hammer, Ø., Harper, D. A. T. & Ryan, P. D. PAST: Paleontological statistics software package for education and data analysis. *Palaeontol. Electron.* **4**, 1–9 (2001).
20. CLSI. *Susceptibility Testing of Mycobacteria, Nocardiae, and Other Aerobic Actinomycetes* (Clinical and Laboratory Standards Institute, 2018).
21. Vega, D., Moreno, J. E. & Mansilla, E. C. Methods for determining the antimicrobial susceptibility of mycobacteria. (2016).
22. Mohanta, T. & Goel, S. Prevalence of antibiotic-resistant bacteria in three different aquatic environments over three seasons. *Environ. Monit. Assess.* **186**, 5089–5100. https://doi.org/10.1007/S10661-014-3762-1 (2014).
23. Klein, E. Y., Tseng, K. K., Pant, S. & Laxminarayan, R. Tracking global trends in the effectiveness of antibiotic therapy using the Drug Resistance Index. *BMJ Glob Heal*. **4**, e001315. https://doi.org/10.1136/BMJGH-2018-001315 (2019).
24. Heuer, H., Krsek, M., Baker, P., Smalla, K. & Wellington, E. M. H. Analysis of actinomycete communities by specific amplification of genes encoding 16S rRNA and gel-electrophoretic separation in denaturing gradients. *Appl. Environ. Microbiol.* **63**, 3233. https://doi.org/10.1128/AEM.63.8.3233-3241.1997 (1997).
25. Ghyselinck, J., Pfeiffer, S., Heylen, K., Sessitsch, A. & De Vos, P. The Effect of Primer Choice and Short Read Sequences on the Outcome of 16S rRNA Gene Based Diversity Studies. *PLoS One*. **8**, e71360. https://doi.org/10.1371/JOURNAL.PONE.0071360 (2013).
26. Ledesma, Y. et al. The Re-Identification of Previously Unidentifiable Clinical Non-Tuberculous Mycobacterial Isolates Shows Great Species Diversity and the Presence of Other Acid-Fast Genera. *Pathogens* **11**, 1159. https://doi.org/10.3390/PATHOGENS11101159/S1 (2022).
27. Swofford, D. L. PAUP*. Phylogenetic Analysis Using Parsimony (*and Other Methods). (2002).
28. Kumar, S., Stecher, G., Li, M., Knyaz, C. & Tamura, K. MEGA X: Molecular Evolutionary Genetics Analysis across Computing Platforms. *Mol. Biol. Evol.* **35**, 1547–1549. https://doi.org/10.1093/MOLBEV/MSY096 (2018).
29. Sharma, S., Upadhyay, V. & Epidemiology diagnosis & treatment of non-tuberculous mycobacterial diseases. *Indian J. Med. Res.* **152**, 185. https://doi.org/10.4103/IJMR.IJMR_902_20 (2020).
30. Nasre-Nasser, R. & Muñoz-López, G. Mycobacterium scrofulaceum infection in a pediatric patient from the Galapagos Islands - Ecuador. *Rev. Chil. infectología*. **35**, 705–709. https://doi.org/10.4067/S0716-10182018000600705 (2018).
31. Palacios Vargas, D. V. Mycobacterium terrae: case report. Rev Ecuatoriana Ciencia, Tecnol e Innovación en Salud Pública. ;:1–4. (2021). https://doi.org/10.31790/inspilip.v5i2.219
32. Moreno-Izquierdo, C., Zurita, J., Contreras-Yametti, F. I. & Jara-Palacios, M. A. Mycobacterium abscessus subspecies abscessus infection associated with cosmetic surgical procedures: Cases series. *IDCases* 22. https://doi.org/10.1016/J.IDCR.2020.E00992 (2020).
33. Romero, J. J. et al. Panniculitis caused by Mycobacterium monacense mimicking erythema induratum: A case in Ecuador. *New. Microbes New. Infect.* **10**, 112–115. https://doi.org/10.1016/j.nmni.2016.01.006 (2016).
34. Dohál, M., Porvazník, I., Solovič, I. & Mokrý, J. Whole Genome Sequencing in the Management of Non-Tuberculous Mycobacterial Infections. *Microorganisms* 9. https://doi.org/10.3390/MICROORGANISMS9112237 (2021).
35. Kwon, Y. S., Daley, C. L. & Koh, W. J. Managing antibiotic resistance in nontuberculous mycobacterial pulmonary disease: challenges and new approaches. https://doi.org/101080/1747634820191638765. ;13:851–61. (2019). https://doi.org/10.1080/17476348.2019.1638765
36. Kim, S. H. & Shin, J. H. Identification of nontuberculous mycobacteria using multilocous sequence analysis of 16S rRNA, hsp65, and rpoB. *J. Clin. Lab. Anal.* 32. https://doi.org/10.1002/JCLA.22184 (2018).
37. Gupta, R. S., Lo, B. & Son, J. Phylogenomics and comparative genomic studies robustly support division of the genus Mycobacterium into an emended genus Mycobacterium and four novel genera. Front Microbiol. ;9 FEB:67. (2018). https://doi.org/10.3389/fmicb.2018.00067
38. Brown-Elliott, B. A. & Wallace, R. J. Clinical and taxonomic status of pathogenic nonpigmented or late-pigmenting rapidly growing mycobacteria. *Clin. Microbiol. Rev.* **15**, 716–746. https://doi.org/10.1128/CMR.15.4.716-746.2002 (2002).
39. Lee, M. R. et al. Mycobacterium abscessus complex infections in humans. *Emerg. Infect. Dis.* **21**, 1638–1646. https://doi.org/10.3201/EID2109.141634 (2015).

40. Ganapathy, U. S., Dartois, V. & Dick, T. Repositioning rifamycins for Mycobacterium abscessus lung disease. *Expert Opin. Drug Discov.* **14**, 867. https://doi.org/10.1080/17460441.2019.1629414 (2019).
41. Kim, B. J. et al. Identification of Mycobacterial Species by Comparative Sequence Analysis of the RNA Polymerase Gene (rpoB). *J. Clin. Microbiol.* **37**, 1714. https://doi.org/10.1128/JCM.37.6.1714-1720.1999 (1999).
42. Chopra, S., Matsuyama, K., Hutson, C. & Madrid, P. Identification of antimicrobial activity among FDA-approved drugs for combating Mycobacterium abscessus and Mycobacterium chelonae. *J. Antimicrob. Chemother.* **66**, 1533–1536. https://doi.org/10.1093/JAC/DKR154 (2011).
43. Woodley, C. L., Kilburn, J. O., David, H. L. & Silcox, V. A. Susceptibility of Mycobacteria to Rifampin. *Antimicrob. Agents Chemother.* **2**, 245. https://doi.org/10.1128/AAC.2.4.245 (1972).
44. Sha, W., Weng, X., hua, Xiao, H. & He, G. ping, jun. Investigation of drug-resistance to rifampin and rpoB gene sequence analysis of Mycobacterium abscessus. Zhonghua Jie He He Hu Xi Za Zhi. ;26:544–7. (2003).
45. Lambert, P. A. Cellular impermeability and uptake of biocides and antibiotics in Gram-positive bacteria and mycobacteria. *J. Appl. Microbiol.* **92**, 46S–54. https://doi.org/10.1046/J.1365-2672.92.5S1.7.X (2002). S.
46. Adékambi, T., Drancourt, M. & Raoult, D. The rpoB gene as a tool for clinical microbiologists. *Trends Microbiol.* **17**, 37–45. https://doi.org/10.1016/J.TIM.2008.09.008 (2009).
47. Cuevas-Córdoba, B. et al. A bioinformatics pipeline for Mycobacterium tuberculosis sequencing that cleans contaminant reads from sputum samples. *PLoS One*. **16**, e0258774. https://doi.org/10.1371/JOURNAL.PONE.0258774 (2021).
48. Ho, Y. S. et al. Complete Genome Sequence of Mycobacterium fortuitum subsp. fortuitum Type Strain DSM46621. *J. Bacteriol.* **194**, 6337. https://doi.org/10.1128/JB.01461-12 (2012).
49. Sassi, M. & Drancourt, M. Genome analysis reveals three genomospecies in Mycobacterium abscessus. *BMC Genom.* **15**, 1–10. https://doi.org/10.1186/1471-2164-15-359/FIGURES/4 (2014).
50. Winburn, B. & Sharman, T. Atypical Mycobacterial Disease. StatPearls. (2022).
51. Sakai, T. et al. Expression and role of heat-shock protein 65 (HSP65) in macrophages during Trypanosoma cruzi infection: involvement of HSP65 in prevention of apoptosis of macrophages. *Microbes Infect.* **1**, 419–427. https://doi.org/10.1016/S1286-4579(99)80045-8 (1999).
52. Ferrell, K. C., Johansen, M. D., Triccas, J. A. & Counoupas, C. Virulence Mechanisms of Mycobacterium abscessus: Current Knowledge and Implications for Vaccine Design. *Front. Microbiol.* **13**, 557. https://doi.org/10.3389/FMICB.2022.842017/BIBTEX (2022).
53. Roux, A. L. et al. The distinct fate of smooth and rough Mycobacterium abscessus variants inside macrophages. *Open. Biol.* 6. https://doi.org/10.1098/RSOB.160185 (2016).
54. Clarridge, J. E. Impact of 16S rRNA Gene Sequence Analysis for Identification of Bacteria on Clinical Microbiology and Infectious Diseases. *Clin. Microbiol. Rev.* **17**, 840. https://doi.org/10.1128/CMR.17.4.840-862.2004 (2004).
55. Zhou, L. et al. A new single gene differential biomarker for mycobacterium tuberculosis complex and non-tuberculosis mycobacteria. Front Microbiol. ;10 AUG:1887. (2019). https://doi.org/10.3389/FMICB.2019.01887/BIBTEX
56. Zelazny, A. M. et al. Cohort study of molecular identification and typing of Mycobacterium abscessus, Mycobacterium massiliense, and Mycobacterium bolletii. *J. Clin. Microbiol.* **47**, 1985–1995. https://doi.org/10.1128/JCM.01688-08 (2009).
57. Adékambi, T., Berger, P., Raoult, D. & Drancourt, M. rpoB gene sequence-based characterization of emerging non-tuberculous mycobacteria with descriptions of Mycobacterium bolletii sp. nov., Mycobacterium phocaicum sp. nov. and Mycobacterium aubagnense sp. nov. *Int. J. Syst. Evol. Microbiol.* **56** (Pt 1), 133–143. https://doi.org/10.1099/IJS.0.63969-0 (2006).
58. Borek, A., Zabost, A., Głogowska, A., Filipczak, D. & Augustynowicz-Kopeć, E. New RAPMYCOI SensititreTM Antimicrobial Susceptibility Test for Atypical Rapidly Growing Mycobacteria (RGM). *Diagnostics (Basel Switzerland)*. 12. https://doi.org/10.3390/DIAGNOSTICS12081976 (2022).
59. Ringuet, H. et al. hsp65 sequencing for identification of rapidly growing mycobacteria. *J. Clin. Microbiol.* **37**, 852–857. https://doi.org/10.1128/JCM.37.3.852-857.1999 (1999).
60. Kim, H. et al. Differentiation of Myocobacterium species by analysis of the heat-shock protein 65 gene (hsp65). *Int. J. Syst. Evol. Microbiol.* **55**, 1649–1656. https://doi.org/10.1099/IJS.0.63553-0/CITE/REFWORKS (2005).
61. Kim, B. J., Hong, S. H., Kook, Y. H. & Kim, B. J. Molecular Evidence of Lateral Gene Transfer in rpoB Gene of Mycobacterium yongonense Strains via Multilocus Sequence Analysis. *PLoS One*. **8**, 51846. https://doi.org/10.1371/JOURNAL.PONE.0051846 (2013).

Figures

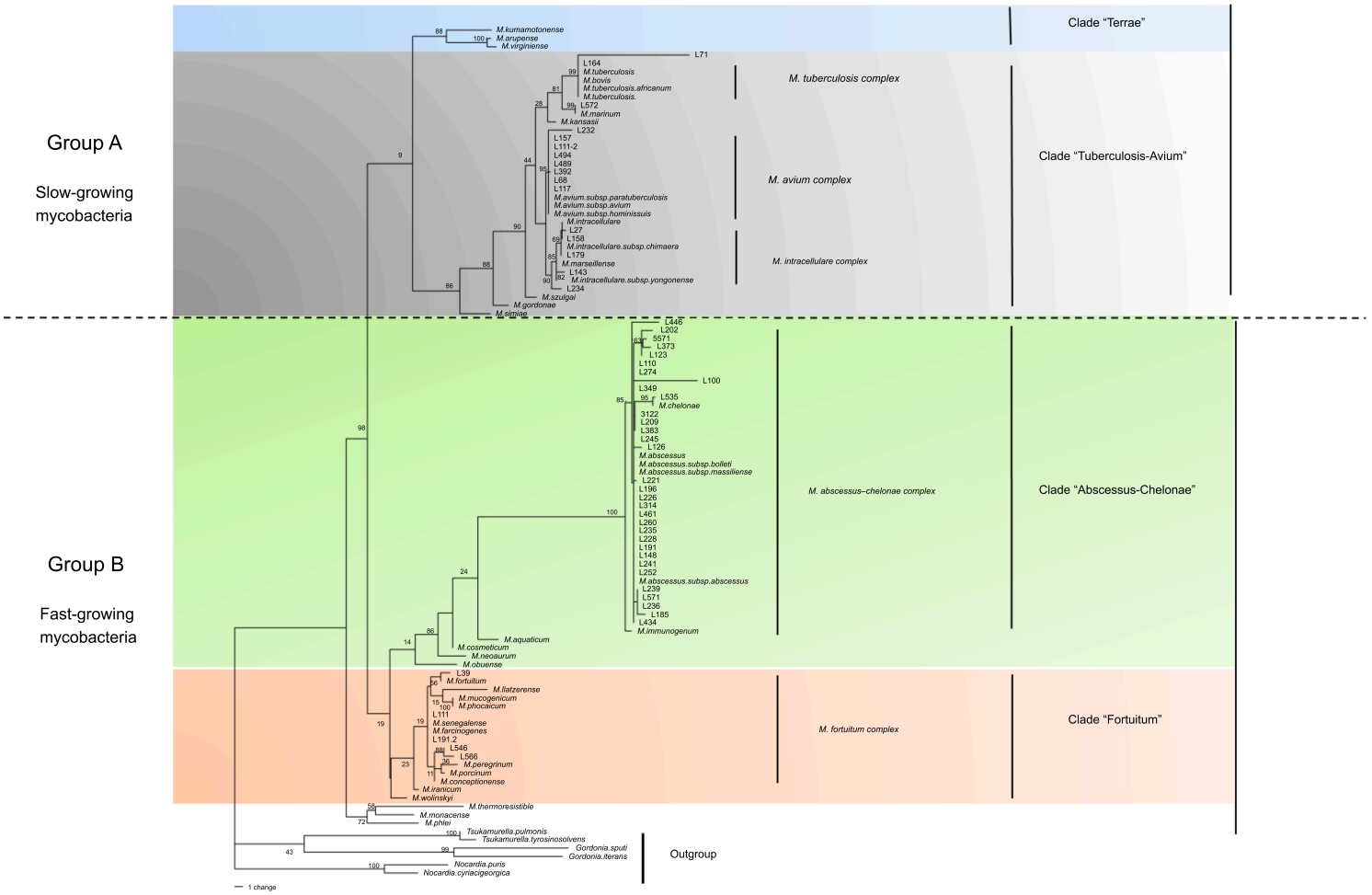


Figure 1

Phylogenetic analysis of the 16S rRNA gene of *Mycobacterium*species. The bars to the right of the tree show the correlation between the monophyletic groups and the natural classification by species complexes, big clades and growth type. Additionally, the colors reinforce the correlation of the lineages with the large-scale classification. The statistical values (%) of bootstrap support are shown on the branches. The base of the tree is rooted with outgroups. The lower bar shows the relationship between evolutionary lines and the number of mutations.

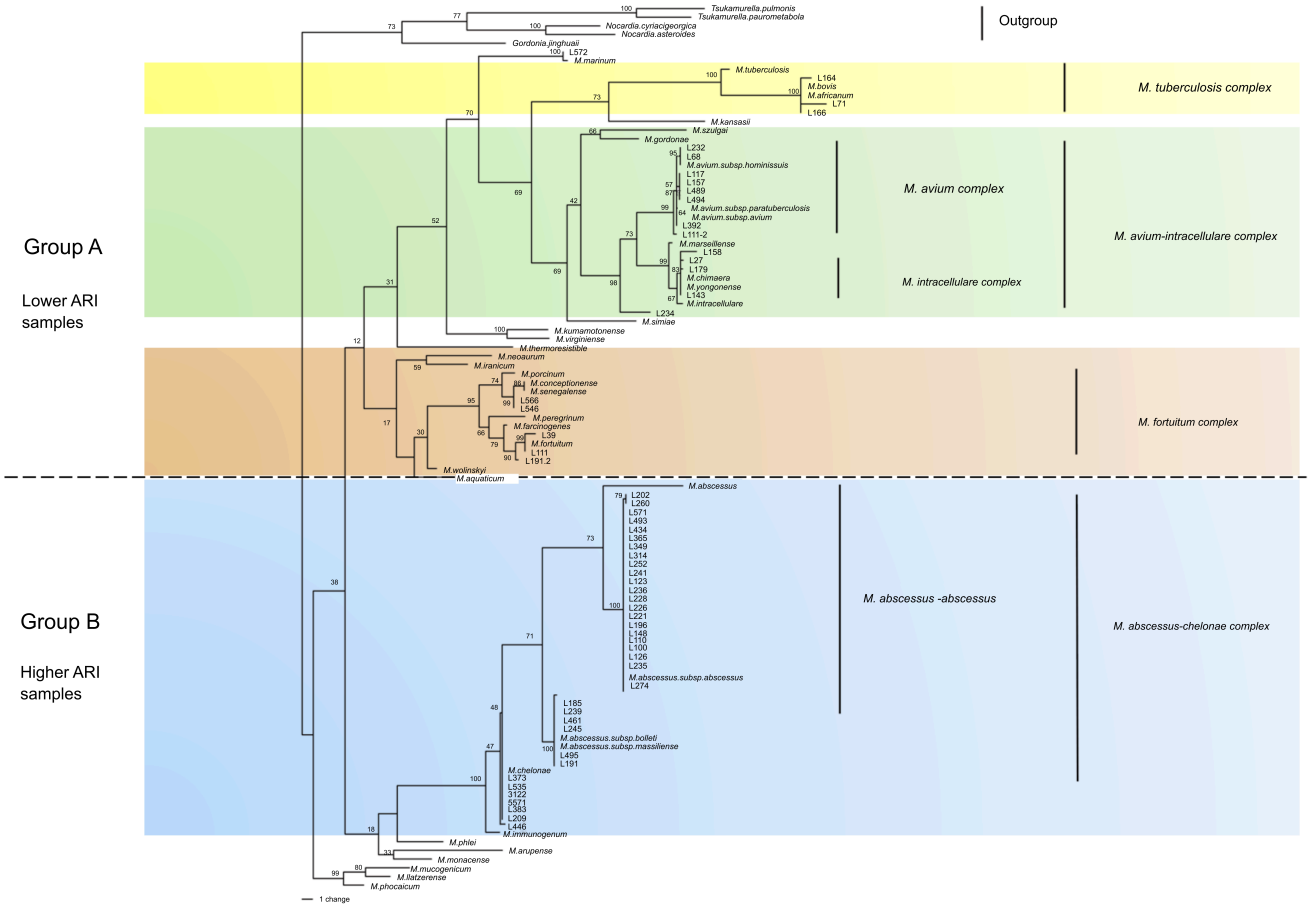


Figure 2

Phylogenetic analysis of the *rpo*B gene of *Mycobacterium*species. The bars to the right of the tree show the correlation between the monophyletic groups and the natural classification by species complexes. Additionally, the colors reinforce the correlation of the lineages with the large-scale classification. Discontinuous lines show the two big lineages A and B (higher ARI value). The statistical values (%) of bootstrap support are shown on the branches. The base of the tree is rooted with outgroups. The lower bar shows the relationship between evolutionary lines and the number of mutations.

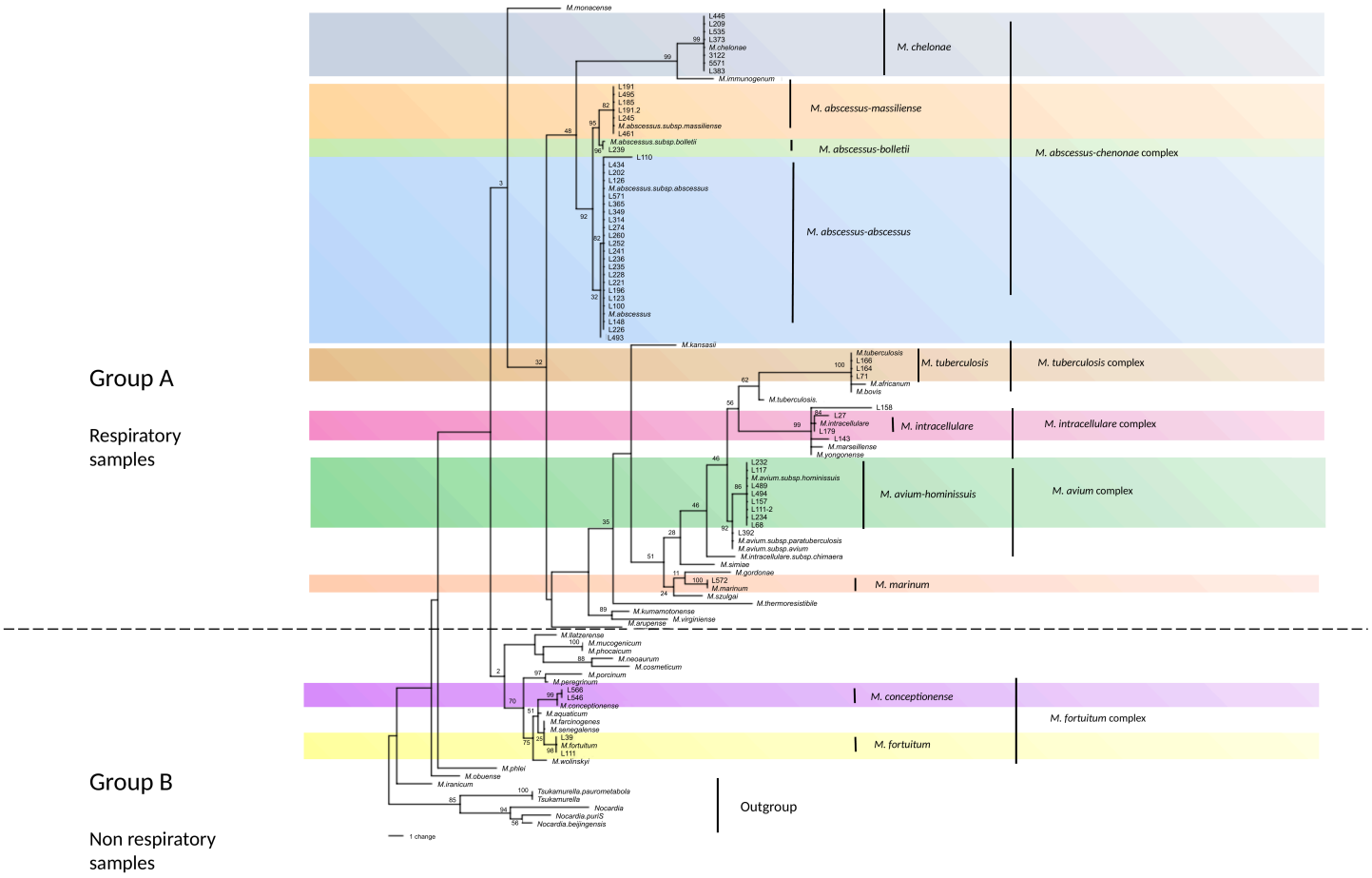


Figure 3

Phylogenetic analysis of the *hsp*65 gene of*Mycobacterium* species.The bars to the right of the tree show the correlation between the monophyletic groups and the natural classification by species complexes. Additionally, the colors reinforce the correlation of the lineages with the large-scale classification. Discontinuous lines shown the two big lineages A (respiratory samples) and B (non-respiratory samples). The statistical values (%) of bootstrap support are shown on the branches. The base of the tree is rooted with outgroups. The lower bar shows the relationship between evolutionary lines and the number of mutations.

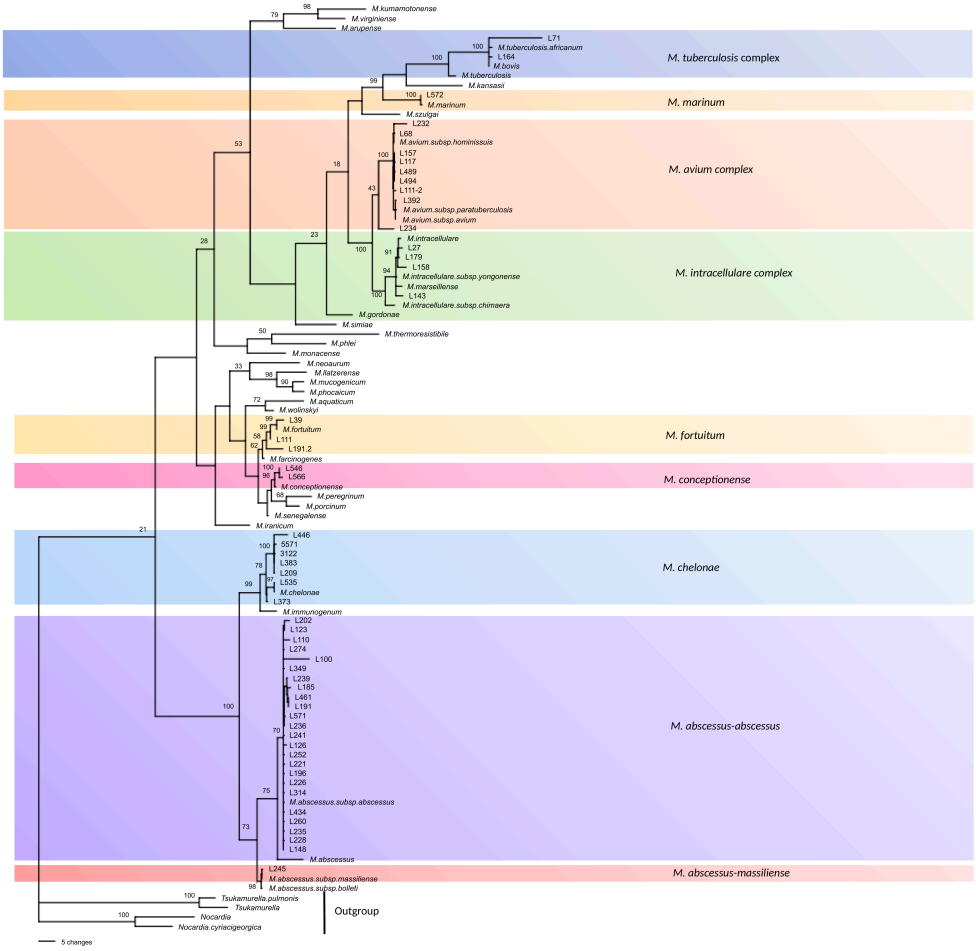


Figure 4

Multilocus sequence analysis (MLSA) of *Mycobacterium*species based on concatenated 16S rRNA, *hsp65*, and *rpoB* gene sequences. The bars to the right of the tree show the correlation between the monophyletic groups and the natural classification by species complexes. Additionally, the colors reinforce the highly recovering lineage of the species/subspecies level. The statistical values (%) of bootstrap support are shown on the branches. The base of the tree is rooted with outgroups. The lower bar shows the relationship between evolutionary lines and the number of mutations

Supplementary Files

This is a list of supplementary files associated with this preprint. Click to download.

- SupplementaryData.docx